Hindawi Publishing Corporation
Active and Passive Electronic Components
Volume 2007, Article ID 78602, 5 pages
doi:10.1155/2007/78602

Research Article

Subwavelength-Diameter Silica Wire and Photonic Crystal Waveguide Slow Light Coupling

Ziyang Zhang,[1] Ulf Andersson,[2] and Min Qiu[1]

[1] *Department of Microelectronics and Applied Physics, Royal Institute of Technology (KTH), Electrum 229, 164 40 Kista, Sweden*
[2] *Center for Parallel Computers, Royal Institute of Technology (KTH), 100 44 Stockholm, Sweden*

Received 28 August 2007; Accepted 21 October 2007

Recommended by Yalin Lu

Counter-directional coupling between subwavelength-diameter silica wire and single-line-defect two-dimensional photonic crystal slab waveguide is studied numerically using parallel three-dimensional finite-different time-domain method. By modifying silica wire properties or engineering photonic crystal waveguide dispersion band, the coupling central wavelength can be moved to the slow light region and the coupling efficiency improves simultaneously. One design gives 82% peak power transmission from silica wire to photonic crystal waveguide over an interacting distance of 50 lattice constants. The group velocity is estimated as 1/35 of light speed in vacuum.

1. INTRODUCTION

There have been extensive studies of slow light in two-dimensional photonic crystal slab waveguide (PCSW) [1–3]. The applications include compact delay lines for photonic signal processing, dispersion management, enhanced light/matter interaction for lasing, and so forth. To couple slow light efficiently, a special interface or a mode converter is usually needed between PCSW and connected dielectric waveguides [4, 5]. Alternatively, we investigate the evanescent counter-directional coupling between subwavelength-diameter silica wire (SiO_2-Wr) and PCSW for slow light generation. A convenient way to draw such SiO_2-Wrs can be found in [6]. There has been previous work on this type of directional coupler [7, 8]. However, the models are mostly two-dimensional and the coupling at slow light region is not investigated. In this paper, we show that the coupling efficiency can be improved greatly when the coupling central wavelength (work point) is moved to the slow light region. The work point can be altered either by changing the refractive index of SiO_2-Wr, or more realistically by modifying the geometries of PCSW. Coupled mode theory is applied to compare the group velocity, coupling efficiency, and coupling bandwidth of the modified PCSWs.

The numerical work is done by parallel three-dimensional finite-difference time-domain method (P3D FDTD). The code, MBfrida, is part of the GEMS suite from Efield AB [9] and is fully parallelized using message passing interface. The simulations are run on Lucidor cluster located at Center for Parallel Computers, Royal Institute of Technology (KTH), Sweden.

2. COUNTER-DIRECTIONAL COUPLING BETWEEN SILICA WIRE AND PHOTONIC CRYSTAL WAVEGUIDE

The schematic of SiO_2-Wr and PCSW directional coupler is shown in Figure 1. The silicon photonic crystal slab has index 3.6 and thickness $0.6a$, where a is the lattice constant. The air-hole diameter is $0.6a$. PCSW is formed by removing one row of air holes along ΓK direction. The PCSW dispersion band can be modified by changing δ, that is, varying the width of the waveguide. For $\delta = 0$, we name the waveguide $PCSW_0$. The index of SiO_2-Wr is 1.5 and the diameter is 1 μm. We choose to place SiO_2-Wr 500 nm above the slab. SiO_2-Wr and $PCSW_0$ are center-aligned in x and go parallel along y. SiO_2-Wr can also be placed on the side of $PCSW_0$ [7]. However, this side coupling risks generating unwanted photonic crystal surface modes [10] and furthermore lowering the coupling efficiency. Another issue is that the photonic crystal lattice between the line-defect and the silica wire is limited to only a few row of air holes in order to achieve sufficient side coupling, This might weaken the in-plane light confinement of $PCSW_0$ and lead to larger propagation loss.

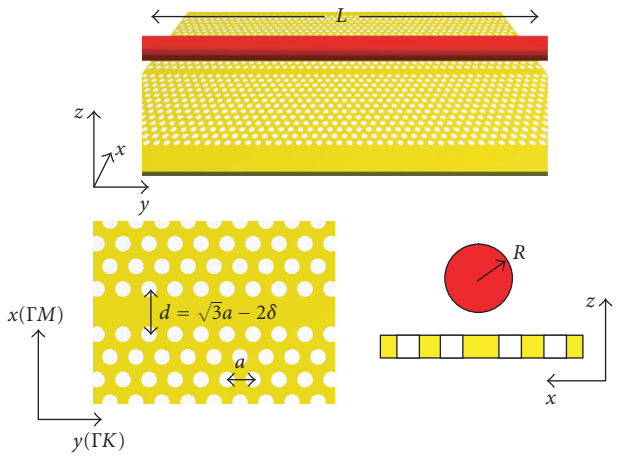

FIGURE 1: Schematic of SiO_2-Wr and PSCW directional coupler.

Figure 2(a) shows the band diagram of $PCSW_0$, calculated using plane wave expansion method (PWE). The zero-order even mode is shown in diamond marker. The fundamental SiO_2-Wr mode dispersion curve is approximately a straight line within the band-gap. Cross point P is the work point, where $PCSW_0$ and SiO_2-Wr share the same propagation constant. The opposite slope sign of the two dispersion curves decides that the evanescent coupling between these two waveguides is counter-directional. Note that since the system is symmetric along x, there is no coupling between fundamental SiO_2-Wr mode and first-order odd $PCSW_0$.

The P3D FDTD transmission simulation is shown in Figure 2(b) with $L = 50a$. The peak power transmission is only 25%, indicating a small coupling coefficient. Also note that the central frequency from P3D FDTD simulation differs slightly from the P point in Figure 2(a). This discrepancy may result from numerical errors in P3D FDTD and PWE methods. Another reason is that the actual dispersion curves for both SiO_2-Wr and $PCSW_0$ are slightly modified for the weakly-coupled system compared to their unperturbed counterparts.

3. SLOW LIGHT GENERATION

We would like to see the coupling behaviour when the work point P moves to the flat band region of PCSW. One easy solution is to change the SiO_2-Wr properties such as wire diameter and material refractive index. For numerical tests we keep the diameter of SiO_2-Wr as 1 μm and change its refractive index from 1.5 to 1.92, 2.0, and 2.1, respectively. The work points move from P_0 to P_1, P_2, and P_3 accordingly, as shown in Figure 3(a). The power simulations are shown in Figure 3(b). As the work point moves further into the slow light region, the peak power transmission goes up, indicating an increase in the coupling coefficient. The coupling bandwidth goes down as the line-width of the transmission spectra decreases.

This interesting phenomenon leads us to more investigation. We keep the index of SiO_2-Wr as 1.5 while modifying PSCW geometry in order to achieve flat-band operation at the coupling point. There are a number of ways to modify the dispersion curve of PSCW. After many trials, we find that one effective way is to reduce the PSCW width d. As shown in Figure 1, $d = \sqrt{3}a - 2\delta$, and we increase δ from 0 to $0.1a$, $0.2a$, and $0.3a$. Accordingly we name the waveguides as $PCSW_0$, $PCSW_1$, $PCSW_2$, and $PCSW_3$. The band diagrams for $PCSW_1$, $PCSW_2$, and $PCSW_3$ are shown in Figure 4. Note that higher-order modes are pulled up from the lower-band edge for these waveguides.

Figure 5 shows the normalised transmission for the modified waveguides in comparison to $PCSW_0$. The coupling length L remains $50a$ for all cases. When $\delta = 0.2a$, the peak transmission reaches 82%. When $\delta = 0.3a$, the coupling with higher-order even mode comes into the frequency window (Q_{III}). From P_0 to P_{II}, we have again observed an improvement of coupling efficiency when the work point moves to the slow light region. At work point P_{III}, the power transmission drops to 58%, despite an increase of group index compared to P_{II}. To understand the coupling behavior better, we have carried out the coupled mode analysis for this system.

4. COUPLED MODE ANALYSIS

We assume weak coupling between SiO_2-Wr mode and PCSW zero-order even mode. At the work point ($\omega = \omega_0$), the power of SiO_2-Wr mode, P_A, and the power of PCSW zero-order even mode, P_B, are related by [11]

$$P_A(y) = P_A(0)\frac{\cosh^2[\kappa(y-L)]}{\cosh^2(\kappa L)}, \qquad P_B(y) = P_A(0)\frac{\sinh^2[\kappa(y-L)]}{\cosh^2(\kappa L)}, \quad 0 \le y \le L. \tag{1}$$

$P_A(0)$ is the input light power from SiO_2-Wr and $P_B(0)$ is the backward transferred (output) power in $PCSW_0$ at the initial point. The coupling coefficient κ is determined by SiO_2-Wr and PCSW vertical spacing as well as their individual mode profile. We define the coupling efficiency η as

$$\eta = \frac{P_B(0)}{P_A(0)} = \frac{\sinh^2(\kappa L)}{\cosh^2(\kappa L)}. \tag{2}$$

The coupling efficiency depends on the product of κ and interacting distance L. When $\kappa L \to \infty$, $\eta \to 1$. For finite κ, complete power transfer from SiO_2-Wr to PCSW is possible when their coupling distance L goes to infinity.

To verify the validity of weak coupling assumptions and (2), we take $\delta = 0.2a$, which gives the highest peak transmission, and vary L from $20a$ to $30a$, $40a$, $50a$, and $70a$. Since the vertical coupling structure is fixed, η is only dependant on L. We run simulations for all cases and take η as the peak value of the power transmission spectra. The values are plotted in Figure 6(a) as discrete data points. The theoretical relation from (2) is plotted as solid curve in Figure 6(a). The average deviation of the simulation values from the theoretic curve is only 3.3%, indicating a good agreement.

Figure 6(b) gives the E_x mode profile in the central slab plane for $PCSW_2$ waveguide first-order even mode (P_{II}) generated from the counter-directional coupling. The power

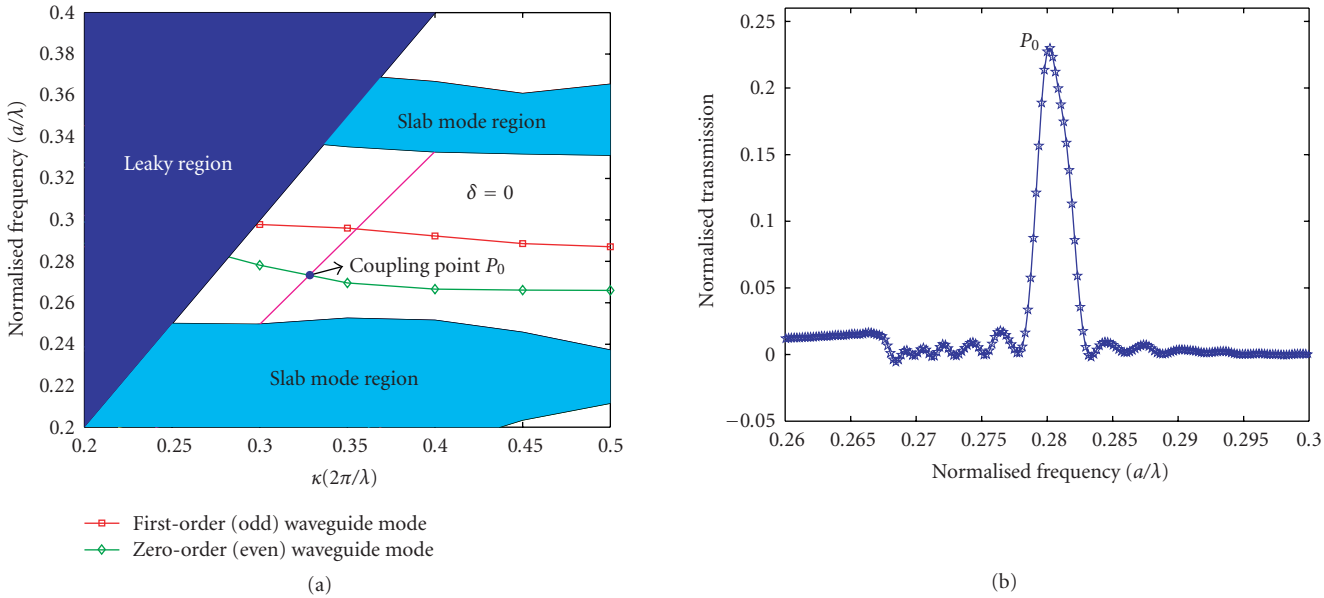

FIGURE 2: (a) Band diagram of $PCSW_0$. The blue curve with diamond marker shows the zero-order even $PCSW_0$ mode. The coupling point is indicated as the blue dot *P*. Due to modal and structural symmetry, SiO_2-Wr mode will not couple with the first-order odd mode of $PSCW_0$ (red curve with square marker). (b) Normalised power transmission in $PSCW_0$ over coupling distance of 50 lattice constants.

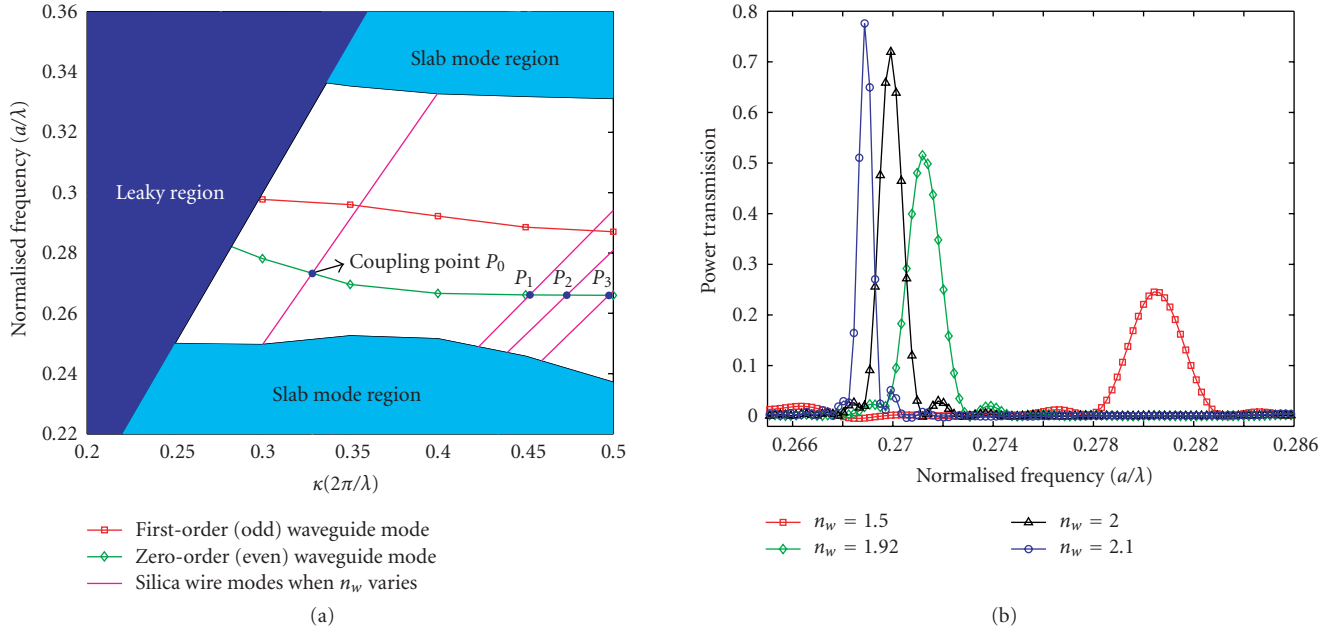

FIGURE 3: (a) The coupling points shift when the refractive index (n_w) of SiO_2-Wr varies from 1.5 (P_0) to 1.92 (P_1), 2.0 (P_2), and 2.1 (P_3). (b) The transmission comparison. As the coupling point moves to the flat band region, the coupling efficiency goes up while the bandwidth shrinks.

TABLE 1: Comparison of $PCSW_{0-3}$

	$PCSW_0$	$PCSW_1$	$PCSW_2$	$PCSW_3(P_{III})$
Peak transmission η	$\eta_0 = 0.25$	$\eta_1 = 0.46 = 1.84\eta_0$	$\eta_2 = 0.81 = 3.24\eta_0$	$\eta_3 = 0.58 = 2.32\eta_0$
Coupling bandwidth $\Delta\omega$ (a/λ)	0.0029	0.0020	0.0013	0.0008
Group index n_g	5.6	12.1	35.0	40.2
Coupling coefficient κ $(a/c/\lambda)$	$\kappa_0 = 0.0064$	$\kappa_1 = 0.0109 = 1.70\kappa_0$	$\kappa_2 = 0.022 = 3.44\kappa_0$	$\kappa_3 = 0.0156 = 2.44\kappa_0$
Figure of merit FOM = n_g $\Delta\omega$	0.0162	0.0242	0.0455	0.0322

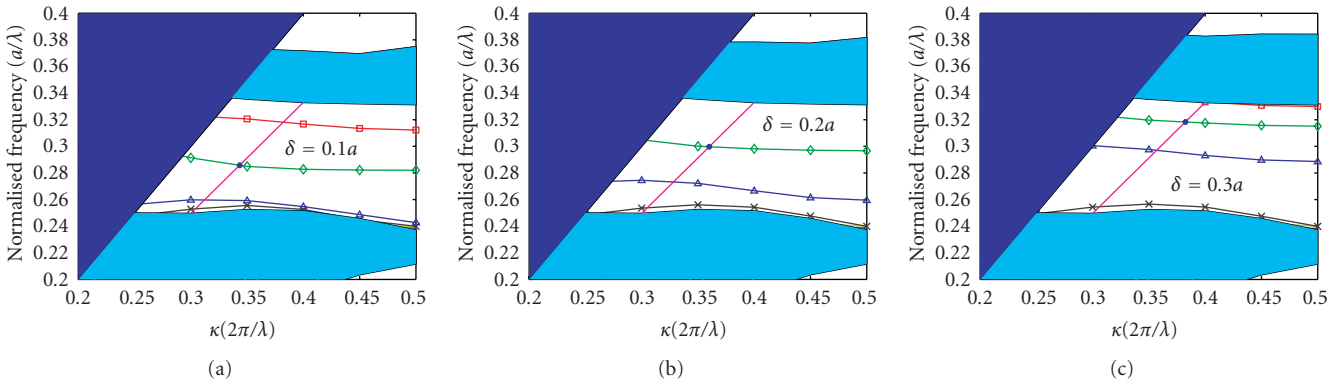

Figure 4: Band diagrams for modified PCSW. (a) $PCSW_1$ with $\delta = 0.1a$; (b) $PCSW_2$ with $\delta = 0.2a$; (c) $PCSW_3$ with $\delta = 0.3a$. Note that higher-order modes (blue curve with triangle marker and black curve with cross marker) are pulled up from the lower band edge.

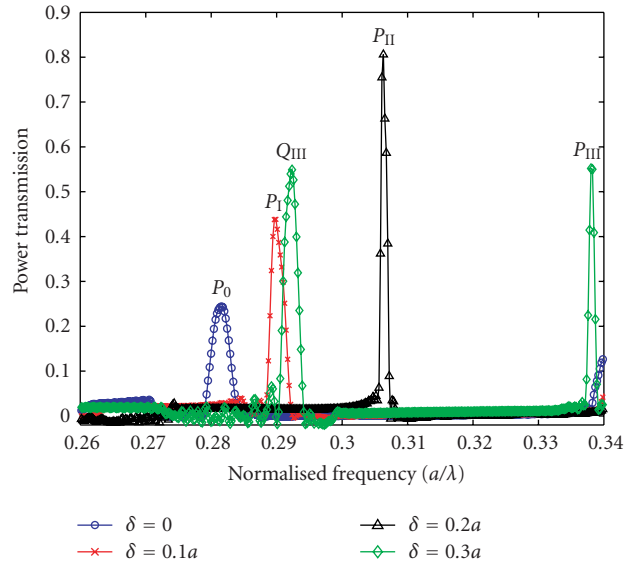

Figure 5: The transmission comparison for modified waveguides. $\delta = 0.2a$ (P_{II}) gives the highest peak transmission, indicating a sharp increase of coupling coefficient. When $\delta = 0.3a$, coupling with higher-order even mode (Q_{III}) comes into the frequency window.

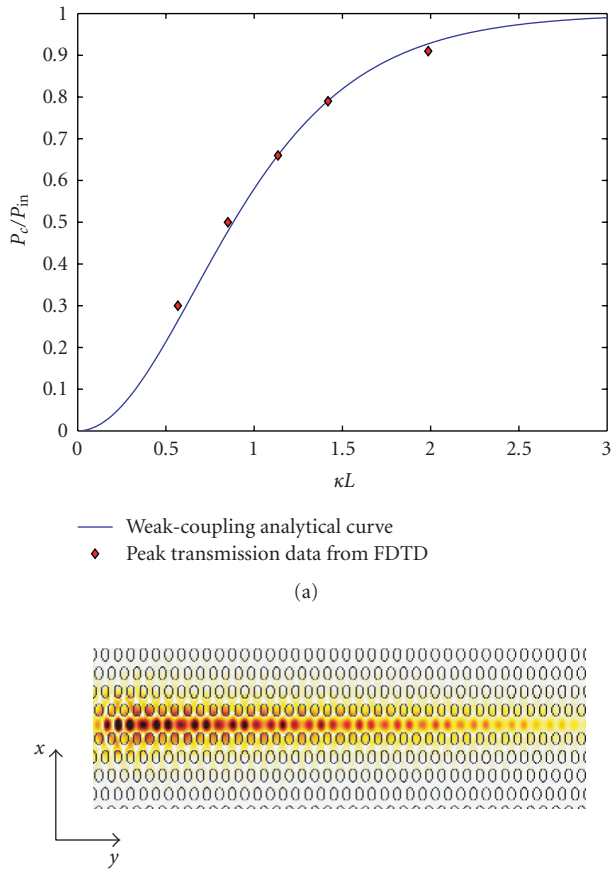

Figure 6: (a) Verification of weak-coupling (2). Only the coupling length L is varied in the $PCSW_2$ case. The peak transmission data from FDTD matches the analytical curve of (2). (b) E_x field profile in $PCSW_2$ generated by counter-directional coupling for $L = 40a$.

flow in the SiO_2-Wr above is along $+y$ direction. The power increases gradually in $PCSW_2$ along $-y$ direction.

From coupled mode theory, the coupling bandwidth $\Delta\omega$ is related to κ and the group velocity v_g of the individual waveguide modes by

$$\Delta\omega = \frac{2\kappa}{1/v_{gB} - 1/v_{gA}} = \frac{2\kappa}{n_{gB} - n_{gA}}c. \quad (3)$$

The group index of SiO_2-Wr mode n_{gA} is 1.2, and n_{gB} is the group index of PCSW mode at coupling point P. The first two rows of Table 1 give the comparison of peak power transmission and coupling bandwidth (full width half maximum) obtained from P3D FDTD simulations, and the third row shows the PCSW group index at the coupling point obtained from PWE method. From the second and third rows of data and (3), the coupling coefficient is calculated. In the last row, we take the figure of merit (FOM) as the product of coupling bandwidth and group index.

From Table 1 and (3), we see that there is a balance between group index and coupling bandwidth in order to

achieve optimal efficiency. Though $PCSW_3$ offers the highest group index at the coupling point, the fast reduction in the coupling bandwidth still brings down the coupling coefficient and the peak transmission. $PCSW_2$ is the preferred design with highest FOM, as well as the best coupling coefficient.

5. SUMMARY

To conclude, we have studied the counter-directional coupling between SiO_2-Wr and PCSW using P3D FDTD simulations and coupled mode analysis. It is shown that the coupling efficiency can be improved by moving the work point into the slow light region. This is achieved by changing the properties of SiO_2-Wr or shortening the width of PCSW. There is also a balance between the coupling bandwidth and group velocity. For $PCSW_2$, the peak power transmission is 82% over 50 lattice constants, and the group velocity is 1/35 of light speed in vacuum. SiO_2-Wrs offer an alternative way to couple slow light efficiently into PCSWs.

ACKNOWLEDGMENTS

This work is supported by the Swedish Foundation for Strategic Research (SSF) through the INGVAR program, the SSF Strategic Research Center in Photonics, and the Swedish Research Council (VR).

REFERENCES

[1] M. Notomi, K. Yamada, A. Shinya, J. Takahashi, C. Takahashi, and I. Yokohama, "Extremely large group-velocity dispersion of line-defect waveguides in photonic crystal slabs," *Physical Review Letters*, vol. 87, no. 25, Article ID 253902, 4 pages, 2001.

[2] H. Gersen, T. J. Karle, R. J. P. Engelen, et al., "Real-space observation of ultraslow light in photonic crystal waveguides," *Physical Review Letters*, vol. 94, no. 7, Article ID 073903, 4 pages, 2005.

[3] L. H. Frandsen, A. V. Lavrinenko, J. Fage-Pedersen, and P. I. Borel, "Photonic crystal waveguides with semi-slow light and tailored dispersion properties," *Optics Express*, vol. 14, no. 20, pp. 9444–9450, 2006.

[4] Y. A. Vlasov and S. J. McNab, "Coupling into the slow light mode in slab-type photonic crystal waveguides," *Optics Letters*, vol. 31, no. 1, pp. 50–52, 2006.

[5] P. Pottier, M. Gnan, and R. M. De La Rue, "Efficient coupling into slow-light photonic crystal channel guides using photonic crystal tapers," *Optics Express*, vol. 15, no. 11, pp. 6569–6575, 2007.

[6] L. Tong, R. R. Gattass, J. B. Ashcom, et al., "Subwavelength-diameter silica wires for low-loss optical wave guiding," *Nature*, vol. 426, no. 6968, pp. 816–819, 2003.

[7] W. Kuang, C. Kim, A. Stapleton, and J. D. O'Brien, "Grating-assisted coupling of optical fibers and photonic crystal waveguides," *Optics Letters*, vol. 27, no. 18, pp. 1604–1606, 2002.

[8] P. E. Barclay, K. Srinivasan, and O. Painter, "Design of photonic crystal waveguides for evanescent coupling to optical fiber tapers and integration with high-*Q* cavities," *Journal of the Optical Society of America B*, vol. 20, no. 11, pp. 2274–2284, 2003.

[9] Efield AB http://www.efieldsolutions.com/.

[10] Z. Zhang, M. Dainese, L. Wosinski, et al., "Optical filter based on two-dimensional photonic crystal surface-mode cavity in amorphous silicon-on-silica structure," *Applied Physics Letters*, vol. 90, no. 4, Article ID 041108, 3 pages, 2007.

[11] A. Yariv, *Optical Electronics in Modern Communications*, chapter 13, Oxford University Press, New York, NY, USA, 5th edition, 1997.